BOLLETTINO DI GEOFISICA TEORICA ED APPLICATA VOL. 44, N. 3-4, PP. 253-279; SEP.-DEC. 2003

Ultrasonic, electric and radar measurements for living trees assessment

L. SAMBUELLI[1], L.V. SOCCO[1], A. GODIO[1], G. NICOLOTTI[2] and R. MARTINIS[2]

[1] *Dipartimento di Georisorse e Territorio, Politecnico di Torino, Italy*
[2] *Dipartimento di Valorizzazione e Protezione delle Risorse Agroforestali, Università di Torino, Italy*

(Received, July 9, 2002; accepted October 31, 2002)

Abstract - The problem of tree assessment is increasingly felt both as a problem of life quality as well as a problem of safety within the city management. One of the main causes of the collapse of a tree is the decay of the bearing capacity of some of the primary roots caused by some kind of fytopathology. This deterioration either changes the physical characteristics of the wood, or changes the water content in the peripheral part of the tree immediately above the ground where the root lies. Experiments have been carried out with regard to these phenomena, to check if one or more geophysical techniques were able to see, with the necessary geometrical and physical resolution, the decay. The techniques tested were: ultrasonic tomography, electric tomography and radar. The problems that arose from the small dimensions of the objects were fixed either increasing the frequency of the testing fields or reducing the size of the probes. The results show very promising possibilities of applications of these quite common geophysical techniques to the non invasive testing of trees, piles and building wood.

1. Introduction

The Visual Tree Assessment (VTA), according to Mattheck and Breloer (1994), consists of three stages: visual inspection of the tree to look for external evidence of internal defects, instrumental measurements of internal defects and evaluation of the residual strength of wood. The instrumental approach suggested by this theory is based on the local evaluation of the velocity of sonic waves generated by "electronic hammers" and on a measurement of wood

Corresponding author: L. Sambuelli, Politecnico di Torino, Dipartimento di Georisorse e Territorio, Corso Duca degli Abruzzi 24, 10129 Torino, Italy. Phone: +39 0115647665, fax: +39 0115647699; e-mail: luigi.sambuelli@potito.it

penetrability using penetrometers. The wide, practical use of the VTA in arboriculture, during these last years, supported a new interest in applying more rapid and precise diagnostic techniques. The most recent methods for a non-invasive evaluation of decay in wood analyse its physical and chemical properties: electrical resistivity (Dubbel et al., 1999; Weihs et al., 1999), modulus of elasticity (Bucur, 1995; Bozhang and Pellerin, 1996; Ross et al., 1997; Berndt et al., 1999), density (Bucur and Archer, 1984; Beall, 1996; Sandoz, 1996; Bucur e Rasolofosaon, 1998; Bucur, 1999), ionic concentration and moisture content (Zoughi, 1990; Smith and Ostrofsky, 1993)

In recent years, there has been an evolution of the instruments applying the aforementioned techniques (Nicolotti and Miglietta, 1998; Godio et al., 1999), often developed for engineering or medical applications, like penetrometers, electrical conductivity meters, ultrasonic detectors, X-rays and γ-rays densimeters (Bucur, 1980; Adjanohoun et al., 1999; Oja, 1999), nuclear magnetic resonance. Most of the instruments designed for investigation of timber, woody structures and wood-based materials, are known as "non destructive" even if it were more appropriate to call them "quasi-non destructive" because, in many cases, probes, electrodes, transducers etc. need to be inserted into the wood. Besides, they give local information influenced by an ill-defined portion of the material surrounding the sensors. Recently, some of these techniques have been developed for tomographic investigation: ultrasonic tomography has been applied by Tomikawa et al. (1990) and Biagi et al. (1994) for investigation of poles and timber, and by Comino et al. (2000b) on living trees; Dubbel et al. (1999), Weihs et al. (1999) and Comino et al. (2000a) carried out many experiments of electric tomography on living trees; Rust and Göcke (2000) designed the PICUS Sonic Tomograph; Temnerud and Oja (1998) and Guddanti and Chang (1998) tested the CT X-rays on logs and Rust (1999) on living trees; tomodensitometry was applied by γ rays on wood by Chambellan et al. (1994). Several studies regard the acoustic-ultrasonic and electrical techniques probably because they are easy to use and require less expensive technology; most of these are applied on timber and woody structures, fewer applications are reported on living trees, particularly with reference to ultrasonic waves.

2. Ultrasonic tomography

Sonic and ultrasonic measurements are well-established, and widely diffuse, surveying techniques for mechanical property assessment of wood lumber or wood-based composite material (Ross and Pellerin, 1994; Beall, 1996; Sandoz, 1996). Theoretical and experimental studies about the acoustics of wood have shown how the velocity of propagation of an ultrasonic pulse can diagnose eventual defects or decreases in strength (Bucur, 1995, 1999; Bozhang and Pellerin, 1996).

In recent years, the possibility of applying the non-invasive techniques, which are typically used for industrial products, to standing trees have stimulated the interest of scientists; and some methods based on sound velocity measurements have been introduced to the practice of tree assessment (Mattheck and Breloer, 1994; Sandoz et al., 2000). Experimental studies have,

in fact, demonstrated that fungal decomposition affects the morphological and mechanical properties of wood (Wilcox, 1978, 1988; Bauer et al., 1991). Usually, fungal decay starts with staining; during this step the wood keeps its mechanical and physical properties. Subsequently, the fungus degrades the components of the wall, reducing the mass, the elastic properties and the internal strength. In particular, the cellulose decomposition causes the major loss of strength in axial fibres and tracheids.

The mostly diffused surveying techniques are based on simple local measurements performed with instrumented hammers. The apparent sonic velocity obtained is usually compared with reference values deducted from literature (Divos, 2000). Some other approaches use the input signal attenuation as a symptom of internal decay or rot (Lawday et al., 2000; Sandoz et al., 2000). Two-dimensional imaging of internal decay has been obtained with a straight ray tomographic inversion of sonic or ultrasonic travel times deducted by an automatic picking procedure (Rust and Gocke, 2000).

Ultrasonic tomography could, in fact, represent an effective tool for decay detection but, since the mechanical behaviour of wood is characterised by strong anisotropy and since ultrasonic pulses in wood are strongly attenuated, great attention has to be devoted both to acquisition and to data processing and interpretation (Comino et al., 2000b; Socco et al., 2000).

Both field experiments, on living trees, and laboratory tests, on samples obtained from the investigated trees, were performed in order to evaluate the effectiveness of ultrasonic tomography for internal decay mapping and to compare tomographic results with the ones obtained by direct measurements. All the data acquisition, analysis and interpretation process can be summarised in the flow-chart of Fig. 1.

3. Data acquisition

The ultrasonic equipment used for data acquisition is a PUNDIT (Portable Ultrasonic Non-destructive Digital Indicating Tester), a single-channel instrument designed for concrete surveying, also suitable for wood investigations. Preliminary tests suggested to adopt exponential probes because their small cross-section allows a better and more local coupling with the bark. The probe operating frequency is 33 kHz. The PUNDIT was connected to an oscilloscope to visualise the signal received in order to perform more accurate travel time readings. Furthermore, in many cases, especially for field measurements, the signal to noise ratio at the receiver probe was quite poor and hence some traces were recorded on a personal computer connected to the oscilloscope, in order to perform further signal processing and to obtain a more reliable first picking.

Fieldwork has mainly consisted of tomographic data acquisition on trees. Measurements were performed in the zone where the VTA inspection and/or other geophysical tests had been previously carried out, or where wood decay was manifest. The tests were carried out on trees of different species and with different trunk geometry (some of them had a quite regular and cylindrical contour while others showed a marked ribbed trunk).

Wood disks were later cut coincident with the measuring sections to check the tomographic

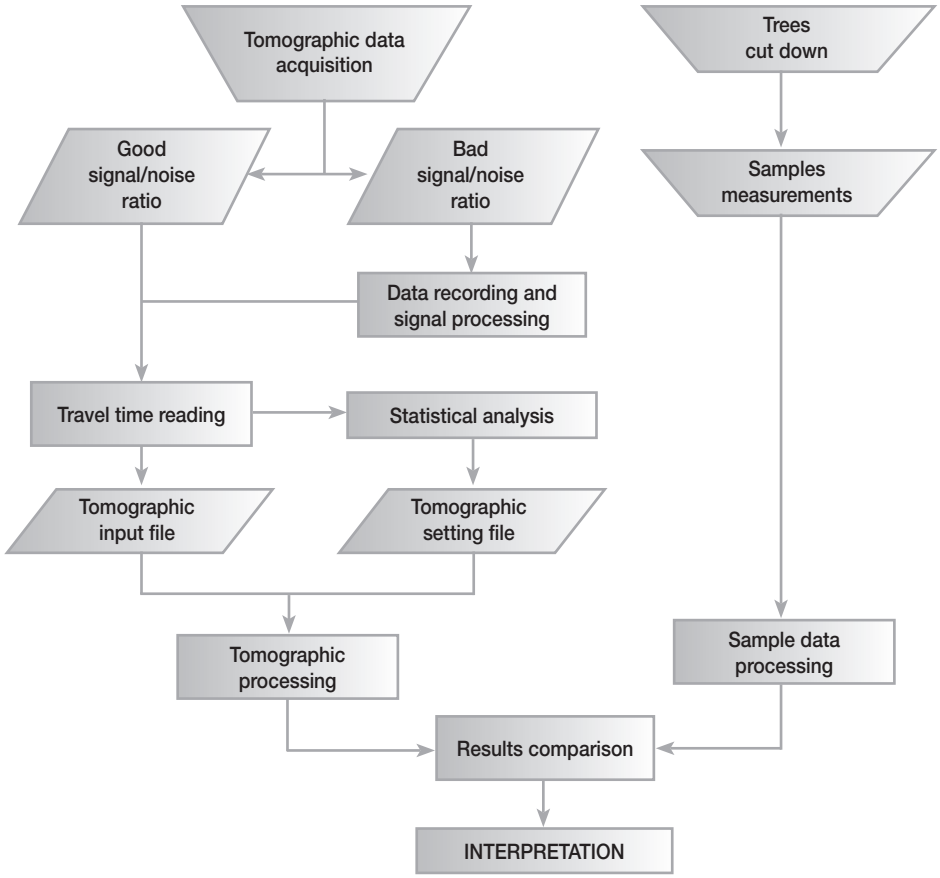

Fig. 1 - Ultrasonic experiments flow-chart.

results and to cut wood samples for laboratory measurements. All the investigated trees showed wood in different stages of fungal decomposition: from staining and discoloration to decay. The white rot fungi, such as the species detected in our samples (*Ganoderma resinaceum Boud.* and *Phellinus tuberculosus Niem.*), are able to degrade the components of the cell wall: lignin, cellulose and hemicellulose.

The measurements on the trunk and on the wood disks were carried out on 16 equidistant points around the investigated section perimeter. Changing the position of the transmitter and receiver probes at each measurement we got 120 independent acquisitions for each tomographic section. The measuring point coordinates were detected by using a simple, specifically designed, mechanical gauge.

Several kinds of laboratory surveys were carried out for each tree: on wood disks, cut from the same section previously measured in the field, and on cubic samples, later extracted from the wood disks. The measurements were carried out to test the feasibility of the ultrasonic acquisition on a trunk with an irregular geometry and to test the ultrasonic sensitivity on early stages of wood decay (Wilcox, 1978, 1988; Bauer et al., 1991). Beside, the laboratory measurements allowed for experimenting background noise conditions lower than outdoor, measurements on wood disks were carried out with tomographic data acquisition with the

same scheme used for field measurements. Whole, healthy disks as well as drilled disks were measured in order to test the sensitivity of the method to small alterations of wood conditions located in eccentric position. Both field and laboratory acquisitions were carried out without barking the wood in order to better simulate the real conditions.

Cubic samples, having the same size as the tomographic cells, were cut along the radial, tangential and longitudinal directions, from the wood disks. The cubic samples were divided into two classes: healthy blocks and decayed blocks (with stained zones and/or white rot). Each specimen was marked by a label, identifying its position in the wood disk, and was hermetically sealed into PVC envelopes to avoid drying. Ultrasonic velocity measurements were performed along the three axes, both on specimens in natural moisture conditions and after drying; moisture content, density, modulus of elasticity and degradation level (weight loss) were also evaluated.

The measurements on cubic samples were carried out not only to assess the tomographic results directly, but also to assess whether the method was capable of discriminating longitudinal, tangential and radial velocity values, in spite of the measuring uncertainty, and to evidence an eventual relation between velocity and sample characteristics, such as the position in the tree section, the presence of wood decay, the presence of bark, and the moisture content.

4. Data processing

After the first arrival picking, which was performed after signal filtering in case of bad signal-to-noise ratio, a criterion to define the uncertainty of data was set both for laboratory and field data.

The difficulty in determining the first arrival of the signal, in some of the acquired traces, stressed the problem of making ultrasonic measurements without barking the tree and also warnes about the reliability of some commercial testing devices performing ultrasonic measurements based on auto-picking procedures (Berndt et al., 2000). On the other hand, it was noticed how, in many cases, exposed wood, showing decay (such as fungi), can be responsible for the great signal attenuation and this could probably be an additional piece of information to take into account (Lawday et al., 2000; Sandoz et al., 2000).

In order to define the reliability of the tomographic interpretation some preliminary data processing was performed both on laboratory and field data. For each S-R (Source-Receiver) couple the value of the average velocity was calculated identifying the ray path with the distance S-R. The time-distance data and the velocity values were used to perform some statistical evaluation in order to estimate the eventual influence of wood anisotropy and the physical resolution of the method.

Anisotropy seems to have a significant effect on measured data. In particular, the average velocity distribution showed, in many cases, a clear bi-modal pattern, that ascertained two velocity values more often occurring in the average velocity population. Where the comparison with laboratory samples was possible, these two velocity values were found very close to the mean velocity values detected on samples along radial and tangential direction respective

(Fig. 2). Furthermore, the displaying of velocity-distance couples, with the associated uncertainties, stressed the eventual effect of anisotropy in tomographic data: shorter ray paths (for closer S-R points) are more influenced by the tangential velocity, while for longer ray paths the radial velocity has a more important role. In some of these graphs, two dominating values of velocity (one for short distances and one for long distances) were highlighted.

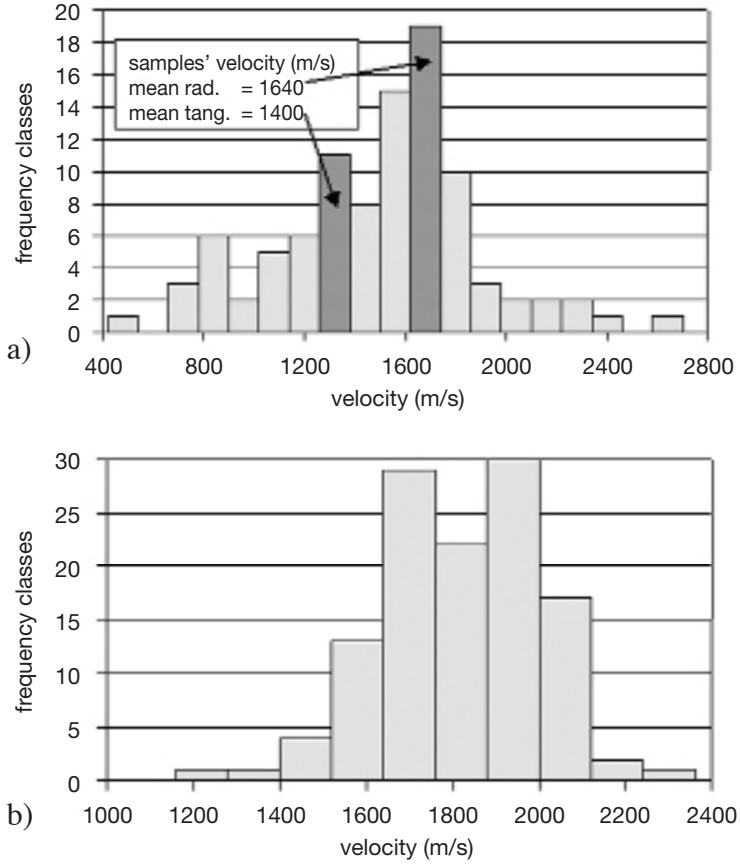

Fig. 2 - Statistical pre-processing of ultrasonic tomographic data: two examples of velocity histograms: a) Hackberry, b) Plane. b) shows a clear bi-modal pattern not so evident in a). It is interesting to notice that for the tree of graph a) the measurements on cubic samples have shown a mean tangential velocity of 1400 m/s and a mean radial velocity of 1640 m/s, corresponding to the two histogram local maxima.

The software MIGRATOM, by USBM (Schneider et al., 1992) was used to process the data. The velocity calculation is performed by a SIRT algorithm and allows for a curved ray tracing (Gilbert, 1972; Dines and Litle, 1979; McGaughey and Young, 1990). Cell size was defined in agreement with both the estimate of the Fresnel radius (Nolet, 1987) and the number of measurements (Menke, 1984). In order to improve result consistency, both global and node constraints on the velocity values were assigned. The global constraints were assigned assuming air velocity as the lower limit and setting the upper velocity limit equal to 150% of the maximum value obtained in the statistical processing (which is actually an apparent value). The

node constraints were used mainly to define the section perimeter imposing the air velocity at the nodes that fall outside the tree contour. Tolerances and the iteration time step were chosen in agreement with the average uncertainty on traveltime data.

5. Laboratory results

The reliability of the visual method to discriminate between sound and decayed wood was confirmed by the weight loss data between the two groups of cubic samples (weight loss 9%). The physical parameters of the healthy and decayed samples (Table 1) show that the mean moisture content is higher in the decayed samples (89%) than in the healthy ones (76%); the weight loss was 9%, and the measured decrease of the dynamic modulus of elasticity was 25%, as reported also by others experiences (Wilcox, 1978). Both the dynamic modulus of elasticity and the velocity of healthy blocks differed significantly in all directions, according to the literature (Giordano, 1981; Beall, 1996; Bucur, 1999). The velocity and the dynamic modulus of elasticity of the decayed blocks did not differ significantly between tangential and radial (Fig. 3).

The longitudinal velocity and dynamic modulus of elasticity were not capable of discriminating between healthy and decayed wood, whilst the tangential and radial values of both these parameters are always significantly different. On fresh wood, the density of healthy and decayed wood is not significantly different whilst there is a difference between healthy and decayed wood in dry conditions. This remark suggested that, on fresh wood, the differences in velocity are mostly related to dynamic elasticity modulus variation rather than density variations. In fact, Giordano (1981) reports a constant trend of dynamic elasticity modulus for moisture contents ranging from the saturation point of fibres to total saturation. In the performed experiments we assume that the modulus differences, between healthy and decayed wood, are related to the elastic property changes due to fungal degradation.

Table 1 - Physical parameters of wood samples. Different letters, between sound and decayed samples, show values significantly different for $P < 0.01$ (ANOVA Tukey HSD test).

	Sound samples (± uncertainty)		**Decayed samples (± uncertainty)**	
	fresh	**dry**	**fresh**	**dry**
Tangential velocity (m/s)	1595 ± 22 b		1322 ± 17 a	
Radial velocity (m/s)	1829 ± 28 c		1550 ± 22 a	
Longitudinal velocity (m/s)	2631 ± 55 d		2486 ± 50 d	
Density (kg/m^3)	966 ± 12 a	640 ± 9 b	941 ± 12 a	568 ± 8 c
Moisture (%)	76 ± 5.6 a		89 ± 16 b	
Basal density (kg/m^3)	551 ± 7 a		504 ± 6 b	
Weight loss [%]	9%			
Tangential Dynamic Elasticity Modulus (MPascal)	2464 ± 75 b		1841 ± 55 a	
Radial Dynamic Elasticity Modulus (MPascal)	3240 ± 107 c		2426 ± 77 a	
Longitudinal Dynamic Elasticity Modulus (MPascal)	6686 ± 293 d		5999 ± 256 d	

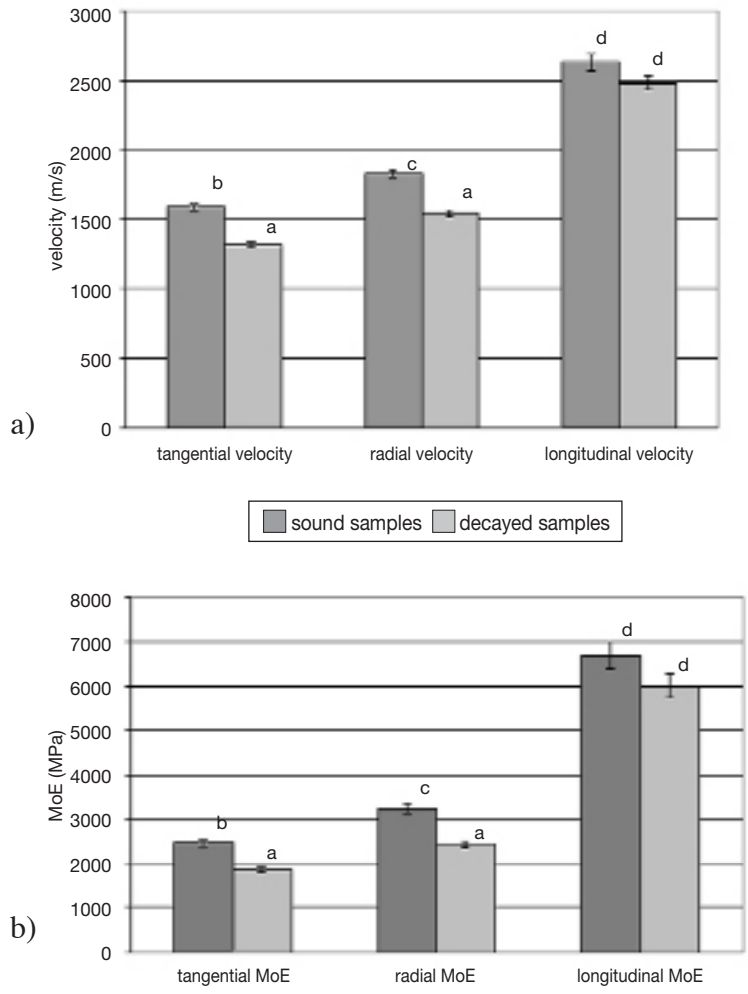

Fig. 3 - Velocity and dynamic modulus of elasticity on healthy and decayed wood. Different letters, between sound and decayed samples, show values significantly different for $P < 0.01$ (ANOVA Tukey HSD test).

6. Tomography results

The results of the tomographic processing showed a very good correspondence between velocity anomalies and wood decay not only on trunks with simple geometry (Fig. 4) but also in case of complex geometry of the trunk and of the decay (Fig. 5). The laboratory experiments on wood disks showed that ultrasonic tomographic imaging could be useful also for monitoring evolving conditions. Tests accomplished on wood disk with small artificial cavities showed that the effect of small targets (with a size of the same order of the spatial resolution) on the tomographic image is often very light. In spite of this, the comparison of the tomographic image of an integer wood disk with the tomographic image obtained by the same wood disk artificially altered, was such that the difference between the images permitted an impressive accuracy in the recognition of quite small anomalies (Fig. 6).

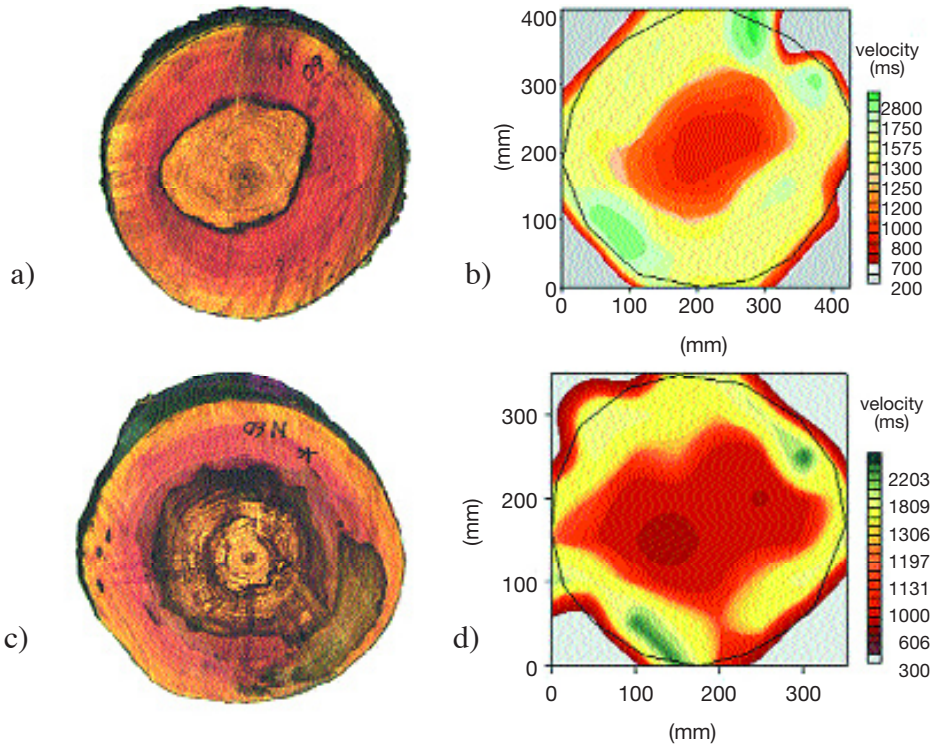

Fig. 4 - Ultrasonic tomographic results on Plane: a) and c) pictures of the investigated sections; b) and d) laboratory tomography on wood disks.

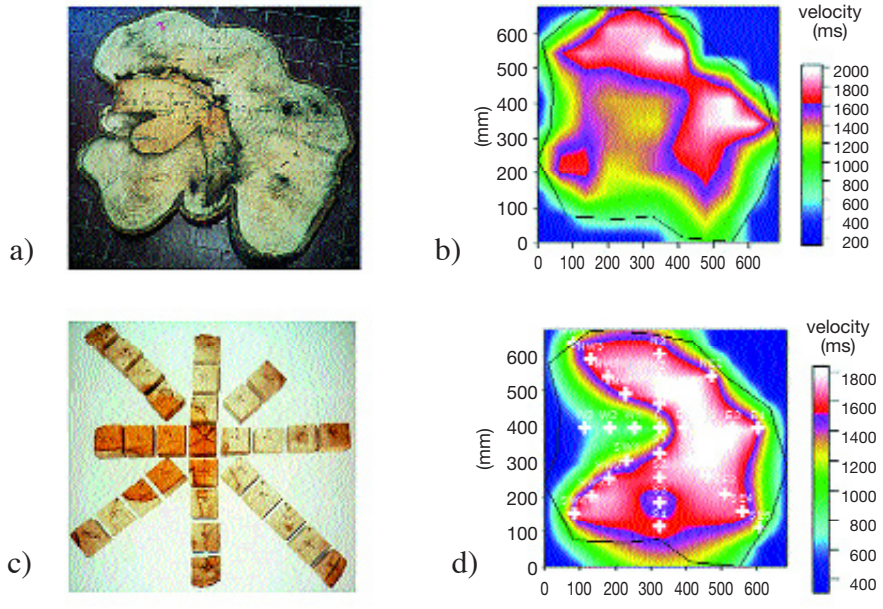

Fig. 5 - Ultrasonic tomographic results on Hackberry: a) picture of the investigated section; b) in situ tomography; c) laboratory samples; d) velocity map obtained by sample measurements (radial - tangential mean velocity). The in situ tomography detected with good resolution the decay even in this case of quite complex geometry; the node constraints allowed reconstruction of the tree perimeter.

A check of the quantitative significance of the tomographic results was possible thanks to the laboratory measurements on cubic samples. Fig. 7 shows a comparison between radial and tangential velocity measured on cubic samples and corresponding velocity value obtained by tomography. Some outliers are due, either to the definition of the tree perimeter or to the fact

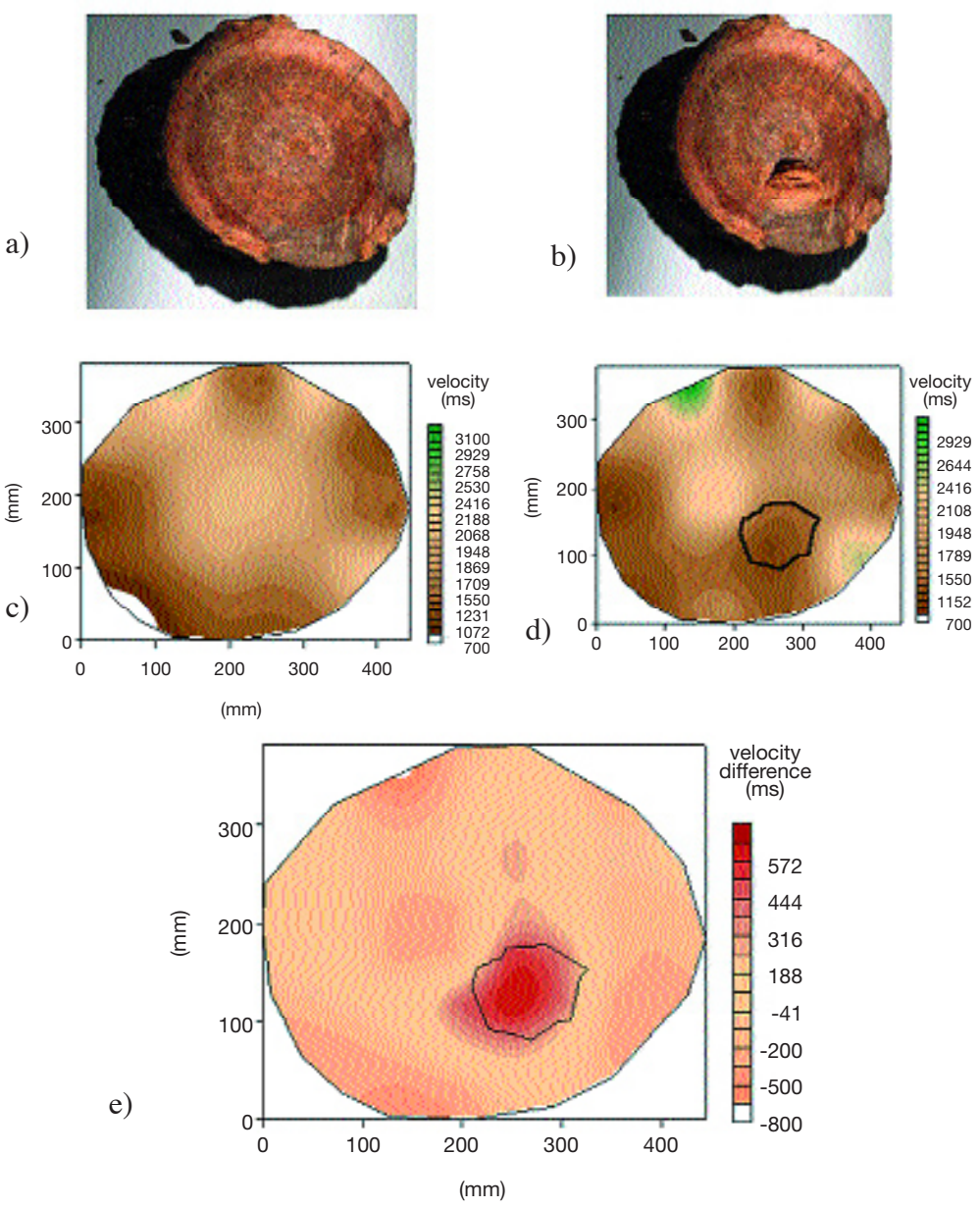

Fig. 6 - Ultrasonic laboratory tomography: a) integer wood disk; b) the same wood disk with a cavity; c) tomographic image of the integer wood disk; d) tomographic image of the wood disk with the cavity; e) difference between the two images. The image d) does not show a significant anomaly while the difference e) clearly evidences the anomaly. The fast zones along the perimeter of the integer wood disk correspond to knots. The slow peripheral zone is probably due to velocity anisotropy.

that they were very peripheral samples (NW4, NE3, NE2, NW4, SE2; see Fig. 5). However, the reliability of the quantitative estimate of the velocity by means of tomography is otherwise confirmed. The velocity decrease due to decay was detected but quite underestimated.

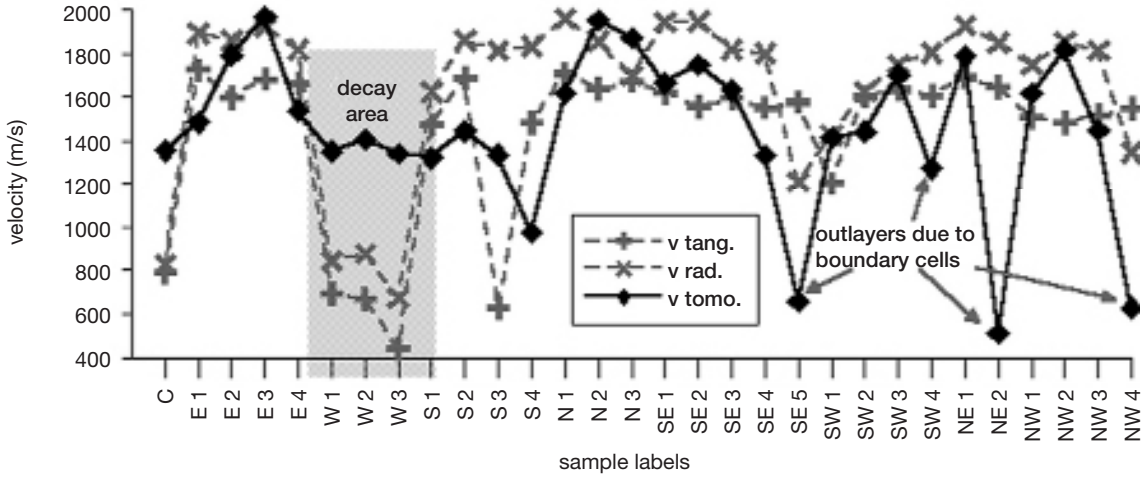

Fig. 7 - Comparison between radial and tangential velocity measured on cubic samples and corresponding velocity value obtained by tomography. Disregarding some outlayers due to the definition of the tree perimeter, the reliability of the quantitative estimate of the velocity by means of tomographic acquisition is confirmed. The velocity decrease due to decay was detected by thetomography but quite underestimated.

7. Electric tomography

The measurements of electrical properties of wood, mainly the resistance, the resistivity and the complex impedance, have been widely used among wood technologists and wood scientists. The main aim of the measurements was either to distinguish the wood type (Blanchard et al., 1983; Smith et al., 1984; Smith and Ostrofsky, 1993) or to find some decays (Blanchard and Tattar, 1974; Sylvia and Tattar, 1976; Smith and Shortle, 1988). More recently (Sandoz e Lorin, 1995), electric measurements have also been used for wooden pole assessments. A good oversight of the theory and of the literature on this subject can be found in Giordano (1981), Skaar (1988), and Torgovnikov (1993). All the aforementioned techniques use two or four electrodes with different lengths (from one centimetre to several centimetres) and different diameters (from around one millimetre to a few millimetres) injecting pulsed or continuous current and measuring a difference of potential. It is well known, in present literature, what kind of problems can arise from the measurement of electrical wood properties and what the order of magnitude of resistance and impedance involved is. However, only in these very last years, with the development of studies around the industrial application of electric or impedance tomography (see, for example, the UMIST web site), a new way of taking electrical measurements on wood has been tried: electric tomography either with resistivity or with capacity measurements (Brownlow White, 1996; Borsic, 1998).

It was decided to explore the possibility of using electric tomography to detect tree decay within a study funded by the municipality of the city of Turin. The research was developed according to the following steps:

1. design and construction of a laboratory device to measure the complex impedance of sound and decayed wood samples;
2. design and construction of a field apparatus with related software to perform electric tomography on trees;
3. experiments of acquisition and processing of electric tomographies on trees that were to be cut down.

8. Laboratory device and tests

An instrument suitable to measure the complex impedance of wood samples in a useful frequency range (10 Hz - 10 MHz) was purposly designed. Two copper square electrodes were connected by a shielded cable to a network analyser. The structure is protected by a metallic cover to prevent anomalies in the measurments due to external electromagnetic fields. Wood samples of the same size as the electrodes, and 7 mm thick, are interposed between the electrodes. Measurements of the complex impedance of wood samples at several frequencies (from 10 Hz to 10 MHz) were carried out. Both real and an imaginary part of impedance, and related uncertainties, were measured to calculate the electrical resistivity, the dielectric constant and the loss angle of healthy and progressivly decayed (*Coniophora puteana*) pine (*Pinus sylvestris*) wood samples. The moisture of the measured samples was quite representative both of a decayed wood (66.8%) and of a dry wood (8.6%) such as the one that can be encountered in the beams of ancient buildings.

Laboratory tests allowed us to define the order of magnitude of the electrical characteristics of wood with different degrees of decay. The estimation of the behaviour both of the real and imaginary part of the impedance of some wood samples drove us to a better selection of operating frequency either in resistivity tomography measurements or in the design of capacitance tomography measurements.

The resistivity vs. frequency graphs (Fig. 8), for example, show that lower frequencies, where the contrast between target and environment is at its maximum (for example below 1 kHz), are more suitable for the detection of either strong decay (high moisture) in a wood beam (dry) or strong decay (high moisture) in a living tree (intermediate moisture). On the other hand, at these lower frequencies, higher electrode impedance is typical so that the measurements become more difficult.

The permittivity vs. frequency graph (Fig. 9) shows some meaningful features. Whichever frequency is used, above approximately 30% of moisture, the graphs tend to overlap to only one curve (see green and red graphs in Fig. 9), hence a kind of water saturation effect can be hypothesized. In literature (Giordano, 1981) a saturation point of water in wood (on average 32% of moisture) is often referred to.

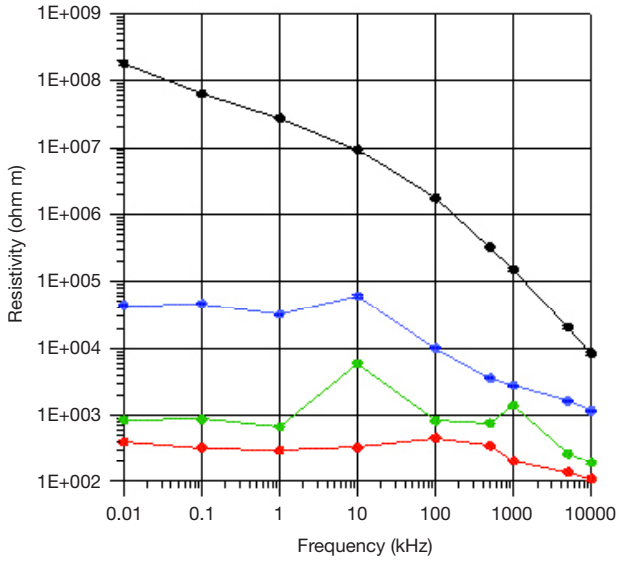

Fig. 8 - Resistivity vs. frequency graphs obtained on specimens with different humidities: black line 8.4%; blue line 27.6%; green line 35.5%; red line 66.8%.

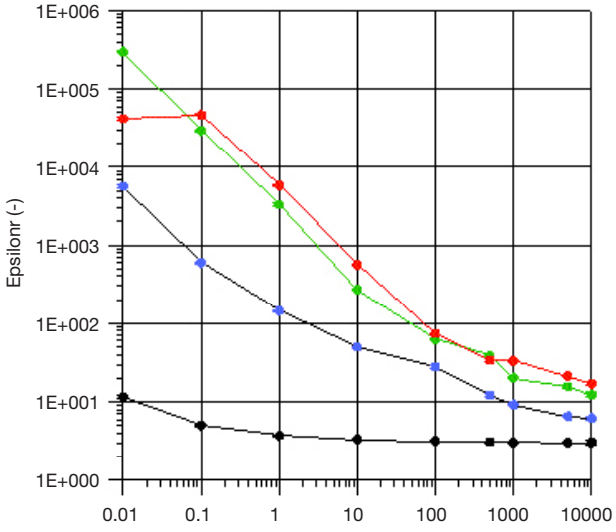

Fig. 9 - Relative electric permittivity vs. frequency graphs obtained on specimens with different humidities: black line 8.4%; blue line 27.6%; green line 35.5%; red line 66.8%.

9. Data acquisition

A purposly designed and crafted instrument has been developed for data acquisition. A digital multimeter is used to measure the potentials. It can be connected to a Personal Computer (PC) via a RS232 link by which it can be programmed and the data can be acquired. The two inputs of the multimeter can be connected, via the multiplexer of the commutation board, to whatever two electrodes on the trunk. The multiplexer also has two other terminals, connected

to the transconductance amplifier, that can also be switched to other two electrodes on the trunk. The signal generator, can inject and pick up a current in the testing object through the transconductance amplifier. The multiplexer of the commutation board is driven via the parallel link of the PC so that it is possible to set up the sequence of current and potential electrodes.

The experiments were carried out with 16 electrodes (on side coated nails 30 mm long and 1.5 mm of diameter) equally spaced around the perimeter; the chosen sequence of energization and reading allowed the collection of 96 independent measurements; the frequency used was 20 Hz.

10. Data processing

It was evident from the theory, the literature, and the case history that the electric tomography images could not have the same quality as those of the nuclear magnetic resonance or of the traditional ecography. It was, therefore, necessary to take the maximum care during the image reconstruction process. The most suitable algorithm to obtain better images with a reasonable computation time seemed to be the quasi-Newton one with a regularisation. The quasi-Newton (Gill et al., 1981; Loke and Barker, 1996; Grootveld et al., 1998) is an iterative algorithm that starts from an estimate of the resistivity distribution and, via a direct algorithm, simulates the measurements that would have been obtained according to such a distribution. After some tests using a finite difference scheme, a finite element approach was chosen for the direct modelling process. At each step the calculated potentials are compared with the experimental ones: if the difference is sufficiently small the process stops (and the last resistivity distribution is taken as the result), otherwise, the resistivity distribution is changed and the potentials are calculated again. From a mathematical point of view the image reconstruction process consists of minimising the following error function:

$$\Phi(\rho^k) = \frac{1}{2}[V(\rho^k) - Vmis]^T [V(\rho^k) - Vmis], \tag{1}$$

where:
$V(\rho^k)$ is the vector of the potential calculated with the direct algorithm at step k,
ρ^k is the vector of the estimated resistivity at step k,
Vmis is the vector of the measured potentials.

The regularisation of the inversion scheme allows a better image reconstruction utilising a-priori knowledge. These latter are used as constraints in the image reconstruction process. A new error function to be minimised is defined:

$$\Phi(\rho^k) = \frac{1}{2}[V(\rho^k) - Vmis]^T [V(\rho^k) - Vmis] + \lambda F(\rho), \tag{2}$$

where $F(\rho)$ can be seen as a penalising function and λ is a multiplication factor. The error function F acts as a constraint on the solution as it assumes higher values in correspondence to undesired values of resistivity. These high values raise the error function so that the minimisation is driven toward acceptable values of resistivity.

The software has been tested twice. First numerically, by modelling an anomalous cylindrical body within a cylindrical background, perturbing the result and inverting the image obtained. This kind of simulation gave very good results as far as the presence and the position of the anomaly are concerned; at this very controlled stage, however, the difficulty of clearly detecting the boundary (the real extension on the section) of the anomaly already came out: some smearing of the contours was, in fact, evident. Second, a physical model was set up: sealed plastic bottles with different diameters were sunk (in various positions) in a water filled cylindrical tank. This controlled analogue simulation also gave good results in positioning the anomalies, and fairly good discrimination within bottles of different diameters. Still there were some uncertainties in determining the real diameters of the anomalous bodies. Edge detection filters were, however, not implemented because a smearing of anomalies contour was likely to occur in real tree measurements.

11. Results

The tests showed the reliability and the good resolution of the method in detecting the geometry of wood decay. Some limitations have been, however, pointed out: a strong variability in electrode contact resistance, affects the reliability of the results; the electrode positions have to be measured with adequate precision otherwise some “ghosts” can appear near the border of the reconstructed image (Fig. 10). In the experiment relative to the images on the top of Fig. 10 the regularity of the trunk perimeter allowed a fairly good reconstruction of the anomaly. On the other hand, in the experiment relative to the images on the bottom of the same figure the protuberance on the left of the trunk produced some artefacts in the left side of the image.

12. Georadar

A ground penetrating radar system has been used to study root systems of trees (Hruska et al., 1999); because of the strong signal attenuation of soils, a low resolution system (antenna of 450 MHz) was adopted. Within this study, the efficiency of georadar (GPR) survey for the 3D reconstruction of the root system of trees in the urban environment and on forest land was checked, with ambiguous results. On the other hand, high resolution GPR measurements appear to be promising for the detection of decayed wood in trees, so that the results of some tests of GPR measurements carried out on standing trees are presented and discussed here. The discussion involves the electromagnetic parameters that control the propagation and attenuation of the electromagnetic signal at the radio-frequency in wood, considering the characteristics and performance of radar equipment. GPR measurements were supported by laboratory analysis of

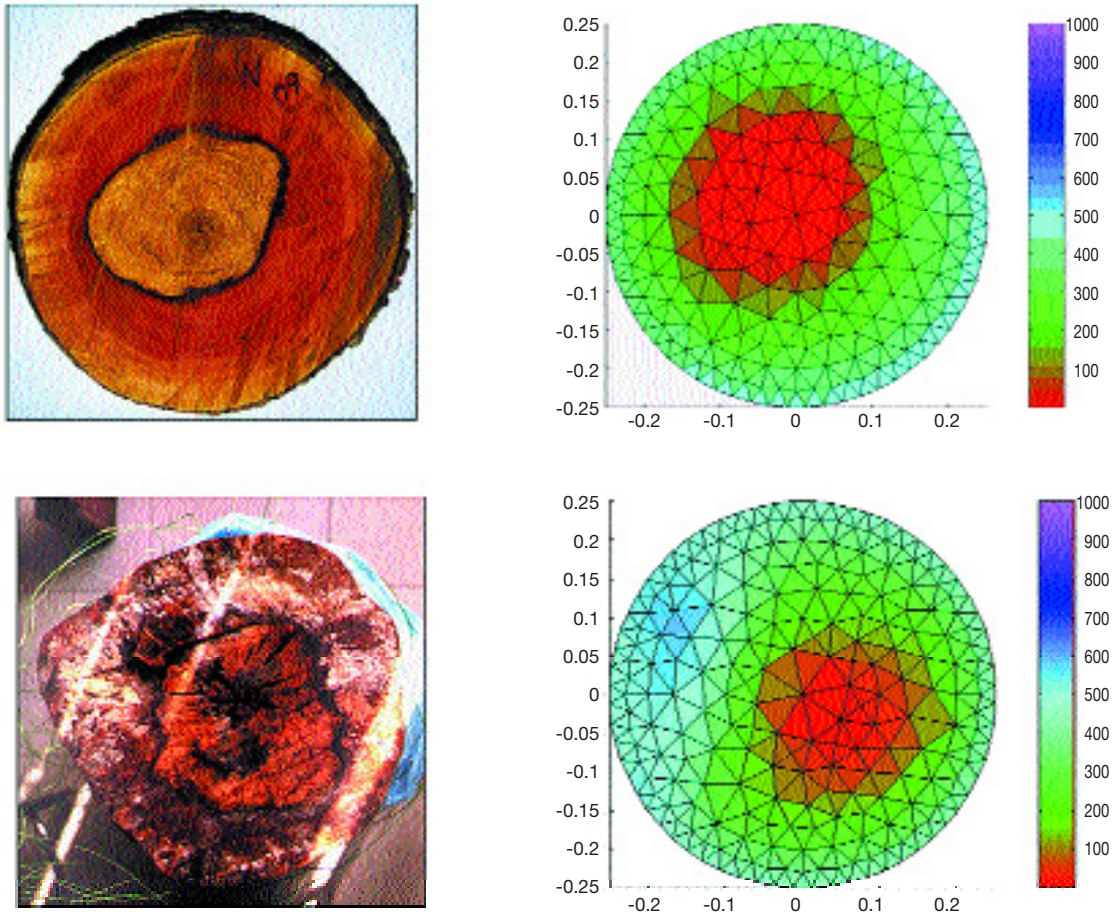

Fig. 10 - Experimental results of electric tomography. Left: trunk disks, right reconstructed tomographic images. The colour scale is normalised.

porosity and water content and measurements of dielectric properties at radar frequencies of different specimens of wood.

GPR surveying on wood consists in acquisition and analysis of signals which are propagated through the wood material and are reflected by anomalies of the electromagnetic properties of wood.

In GPR measurements, to detect the target interface, the signal received must be detectable to the receiver antenna; according to the radar range equation, which defines the maximum distance between the transmitter-receiver antennas and the target (d):

$$SP = 10Log\left[\frac{\upsilon_T \cdot \upsilon_R \cdot G_T \cdot G_R \cdot \lambda^2\, g\Sigma \cdot e^{-4\alpha d}}{64\pi^3 \cdot d^4}\right] \quad (3)$$

where SP (dB) is the system performance parameter, defined as ratio of transmitted power on the minimum detectable power, ν (dimensionless) is the transmitter and receiver efficiency, G (dimensionless) is the transmitter and receiver antenna gain, λ (m) is the signal wavelength in

the medium, g (dimensionless) is the back-scattering gain of target, Σ (m^2) is the target cross sectional area and α (m^{-1}) is the attenuation constant of the medium.

The attenuation constant of the medium at radio-frequency depends on conductivity (s), the complex electromagnetic permittivity and on the radial frequency of the external field. In a low-lossy medium, the imaginary part of the complex permittivity can be sometimes not negligible; for example when high water and salinity content or high degradation of medium occur. In such a context the attenuation rate of material at high frequency (above 1000 MHz) can be very high and the radar range is strongly reduced. The response due to a localised anomaly, such as the one determined by an abrupt change of electromagnetic properties inside the trunk, was approximated with the cross-product of a sphere:

$$g \cdot \Sigma = \pi \cdot r^2 \cdot \Gamma^2, \tag{4}$$

where Γ is the reflection coefficient .

Eq. (3) for a sphere was solved and the radar range for different attenuation rates at frequency of 1000 MHz determined; the results are reported in Fig. 11.

It can be noticed that for high conductivity values of the host medium, the power of the received, reflected signal is below 10 dB beyond 0.2 m from the source; on the other hand, high power reflected signal can be detected up to 0.5 m in wood with low conductivity. Therefore, the performance of radar investigation on wood depends on the electromagnetic properties of bound water and free water (water content, salinity, and mobility of ions) and cell wall components. Modelling the electromagnetic properties, starting from the physical properties of each constituents is a difficult task, because of the complexity of water and ion distributions inside the cells. In such a context, a more general approach is based on the observation that the main

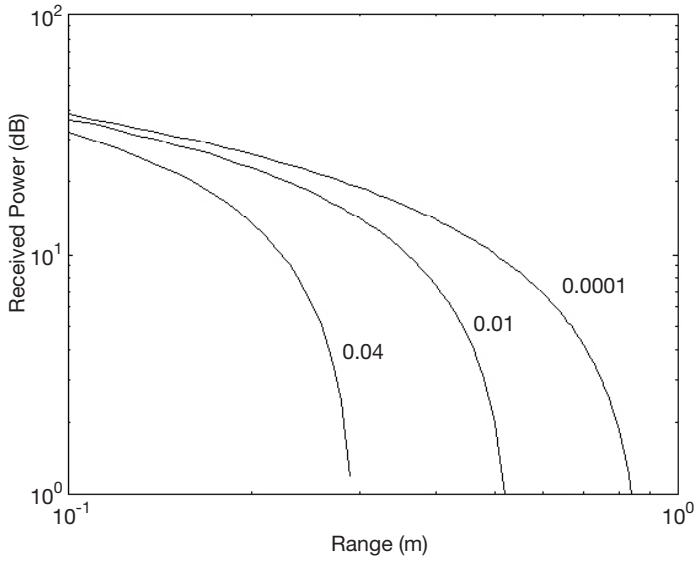

Fig. 11 - Radar range at a frequency of 1000 MHz for different values of conductivity of the host medium for a sphere reflector (radius = 0.05 m).

parameters which affect the electromagnetic properties of the trunk are the total porosity, the total water saturation and the salinity.

The CRIM (Complex Refractive Index Model) model (Birchkak et al., 1974) and other similar models proposed in scientific literature to estimate the electrical permittivity of wood, considers the trunk as a mixture of cell wall, free water, bound water and air (Torgovnikov, 1993); the electric permittivity (real part) of wood samples can be calculated by means of a physical model of wood as multicomponent dielectric:

$$\varepsilon'_m = \left[(1-\phi)\cdot(\varepsilon'_p)^{0.5} + \phi\cdot S_w\cdot(\varepsilon'_w)^{0.5} + \phi\cdot(1-S_w)\cdot(\varepsilon'_a)^{0.5}\right]^2, \tag{5}$$

at the same time,

$$tg\delta_m = \frac{(1-\phi)\cdot(\varepsilon'_p)^{0.5}\cdot tg\delta_p + \phi\cdot S_w\cdot(\varepsilon'_w)^{0.5}\cdot tg\delta_w + (1-S_w)\cdot\phi\cdot(\varepsilon'_a)^{0.5}\cdot tg\delta_a}{(1-\phi)\cdot(\varepsilon'_p)^{0.5} + \phi\cdot(\varepsilon'_w)^{0.5} + (1-S_w)\cdot\phi\cdot(\varepsilon'_a)^{0.5}}, \tag{6}$$

is determined for the imaginary part: where ε'_m, ε'_p, ε'_w, ε'_a are the dielectric constants of medium, dry wood, water, and air; S_w is the relative content of total water in wood and ϕ is the total porosity of the medium.

As reference value for dielectric parameter of single components, we consider $\varepsilon'_w = 80$ (at 20 Celsius degree), $tg\delta_w = 0.06$ (at 1000 MHz) for water components; the cell wall material is non uniform and it is a mixture of substances with different electromagnetic behaviour: cellulose, lignin and resins. A direct measurement of dielectric values of the cell wall is very complex; Torgonivkov (1993) derived some permittivity values for cell wall; he determined, at a frequency of 1000 MHz, permittivity values of $\varepsilon'_c = 3.5$-3.8 (perpendicular to the fibres extent) and $tg\delta_c = 0.05$.

13. Laboratory measurements of electric permittivity

Laboratory measurements of dielectric constant in the frequency range from 200 MHz to 6 GHz have been performed on specimens of different species of trees. The HP 85070B dielectric probe kit was used, with an HP network analyser, controlled by a PC via a GPIB (IEEE488 standard). The measurements were carried out by the contact between the surface of the sample and the probe. The dielectric parameters of the material (real and imaginary part of the electrical permittivity) have been determined from the reflection coefficients at the probe-sample interface (Mosig et al., 1981; Turner et al., 1993).

The accuracy of the measurement of the dielectric constant depends on the frequency of the external electromagnetic field; at frequency below 1 GHz, for samples with low dielectric constant (dry wood), the typical accuracy is in the range of 10 - 20%; at frequency beyond 1 GHz, the accuracy is improved up to 5%. The loss factor and the attenuation rate of the materials can be calculated from the measured real and imaginary part of the dielectric constant. Fig. 12 shows two selected examples of the dielectric constant values measured in

the frequency range of 200 MHz - 6 GHz, for two specimens of sound and decayed wood of *Aesculus hyppocastanum*. A frequency-dependent effect can be observed both in the sound wood and decayed wood; this can not be well separated from the experimental accuracy of the adopted technique which can be very poor at a low frequency. However, the strong difference of permittivity values between sound and decayed wood is justified by the difference in water content of the two specimens: the sound wood was characterised by a moisture of 35% (in weight), while a value of 77% was measured for the decayed wood.

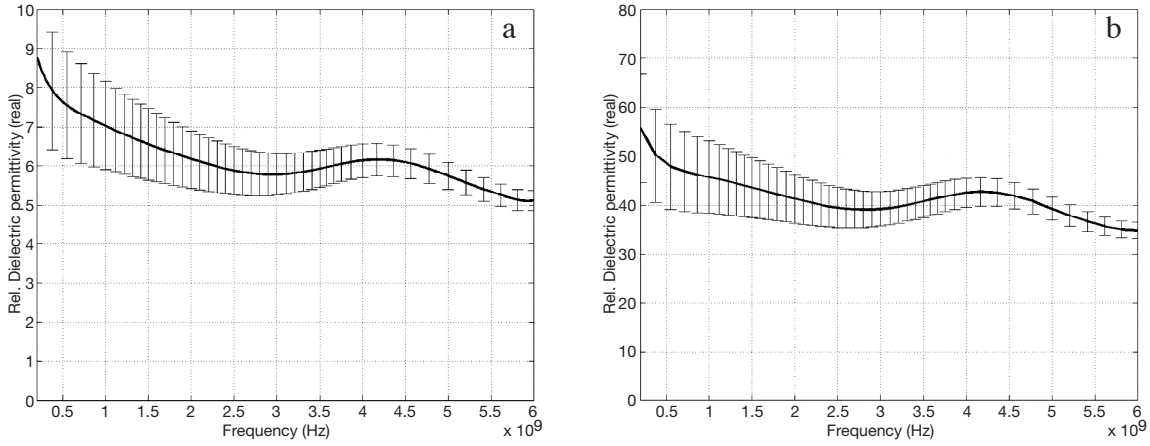

Fig. 12 - Eletrical permittivity (real) of a specimen of wood of *Aesculus* in the frequency range 200 MHz - 6 GHz: a) sound wood; b) decayed wood.

Fig. 13 depicts the results of the modelling of permittivity values, computed on the basis of relationship (5), after the laboratory evaluation of porosity and water saturation values. The values are in the range between 10 and 30; the general trend is an increase of dielectric values from the external part of the section to the core of the plane. In particular, the high dielectric values are well correlated with the inner decayed core of the plane tree. Therefore, a high contrast of electromagnetic impedance between the inner and the outer section is expected. From a theoretical point of view, the interface between the sound and the decayed section of the tree is characterised by strong contrast of the electromagnetic properties and should then be detectable using radar acquisition in reflection modality.

14. Data acquisition

The radar measurements were acquired at different elevations, on the trunk of two trees, moving the antenna along a horizontal perimeter in a single reflection, continuous mode. Tests were performed using 1000 MHz and 1500 MHz main frequency antennas. The main objective of the tests was to evaluate the possibility to correlate the radar reflection events or the signal amplitude anomalies to the decayed and sound zone of the trunk. The evaluation of radar propagation and attenuation can be easily inferred by the analysis of a radar range

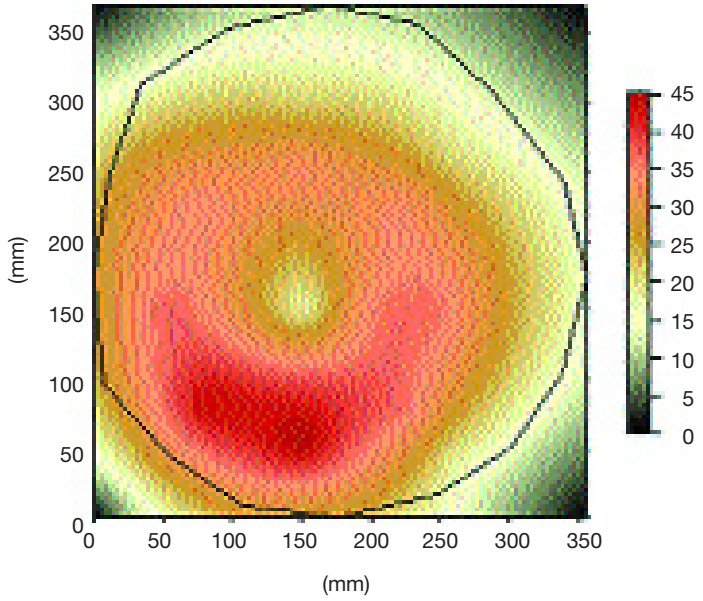

Fig. 13 - Example of theoretical distribution of electrical permittivity (real part) of a tree horizontal section, after measurements of porosity and water content performed on different specimens of the tree section.

equation; more in detail, we can consider the characteristics of resolution of the radar survey in the reflection mode. The vertical resolution is the capability to observe two reflection events as separated along the main signal propagation direction; this depends also on the wavelength (λ) of the propagating wavefield. According to Reynolds (1997) a fairly good estimation of vertical resolution is $\lambda/4$. The spectral analysis and radar wave velocity estimation in wood material permitted to estimate a wave-length of about 6-8 cm, corresponding to a resolution in the radar image of about 2 cm.

15. Data processing

The data processing involved the horizontal (angular) trace normalisation, band pass frequency filtering and horizontal filtering to remove background noise. The final radar sections are represented in polar mode, considering only the time window up to the half-time of the travel-time inside the tree. The lateral resolution is strongly affected by the antenna beam aperture, by the scattering and clustering phenomena due to the coupling between antenna-external surface of the trunk and by the attenuation of radar signal.

16. Results

Two main reflected events are pointed out by radar images of Fig. 14: a first event, close to the external boundary of the tree, is related to the interface between the external low saturated

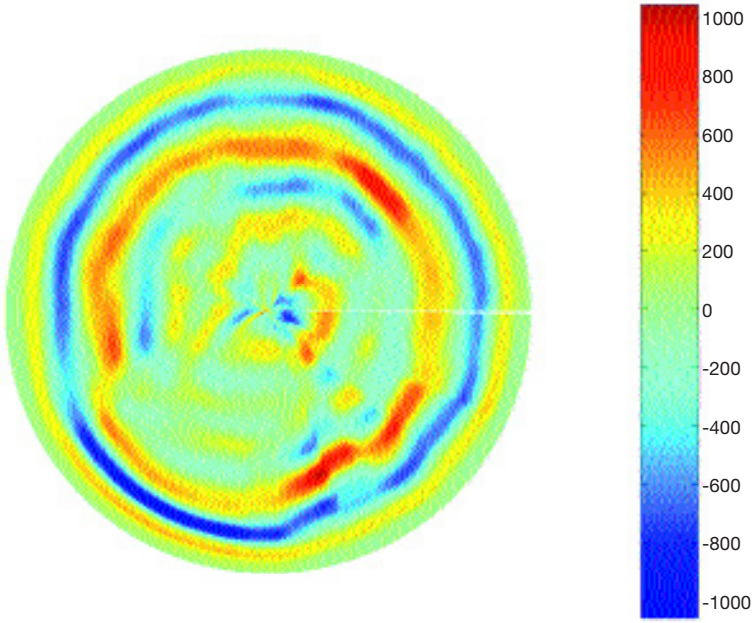

Fig. 14 - Polar georadar images (main frequency of 1500 MHz) for a tree section at 0.2 m from ground level.

zone and the intermediate part of the section; a strong anomaly, in the lower part of the radar image is correlated with the lack in the contrast of electromagnetic impedance of the medium between the external and internal part of the section. The tree is characterised by a gradual change of the electromagnetic properties from the external decayed area to the internal core. The second, main reflected event is related to the interface between the intermediate (high saturated zone) and the internal core with low saturation values. This event well depicts the decayed core of the plane tree.

17. Discussion and conclusion

The three non invasive techniques proposed for standing tree investigation turned out to be effective tools for internal decay detection and characterisation (Fig. 15). Besides this, the quality and the detail of the information obtained are doubtless a significant improvement with respect to the ones achievable by the investigation techniques which are normally used in the practice of tree assessment.

For each of the proposed techniques some critical remarks and some comments are reported in the following, with the aim of emphasising advantages and "open problems".

The ultrasonic tomographic imaging has supplied some impressive results confirming that it could be a powerful non-invasive tool for wood decay detection in living trees. The possibility of accurately detecting the extension of decay, even in the case of very complex shapes of the tree perimeter and of the decay itself, makes this technique a considerable improvement with respect to traditional surveying techniques.

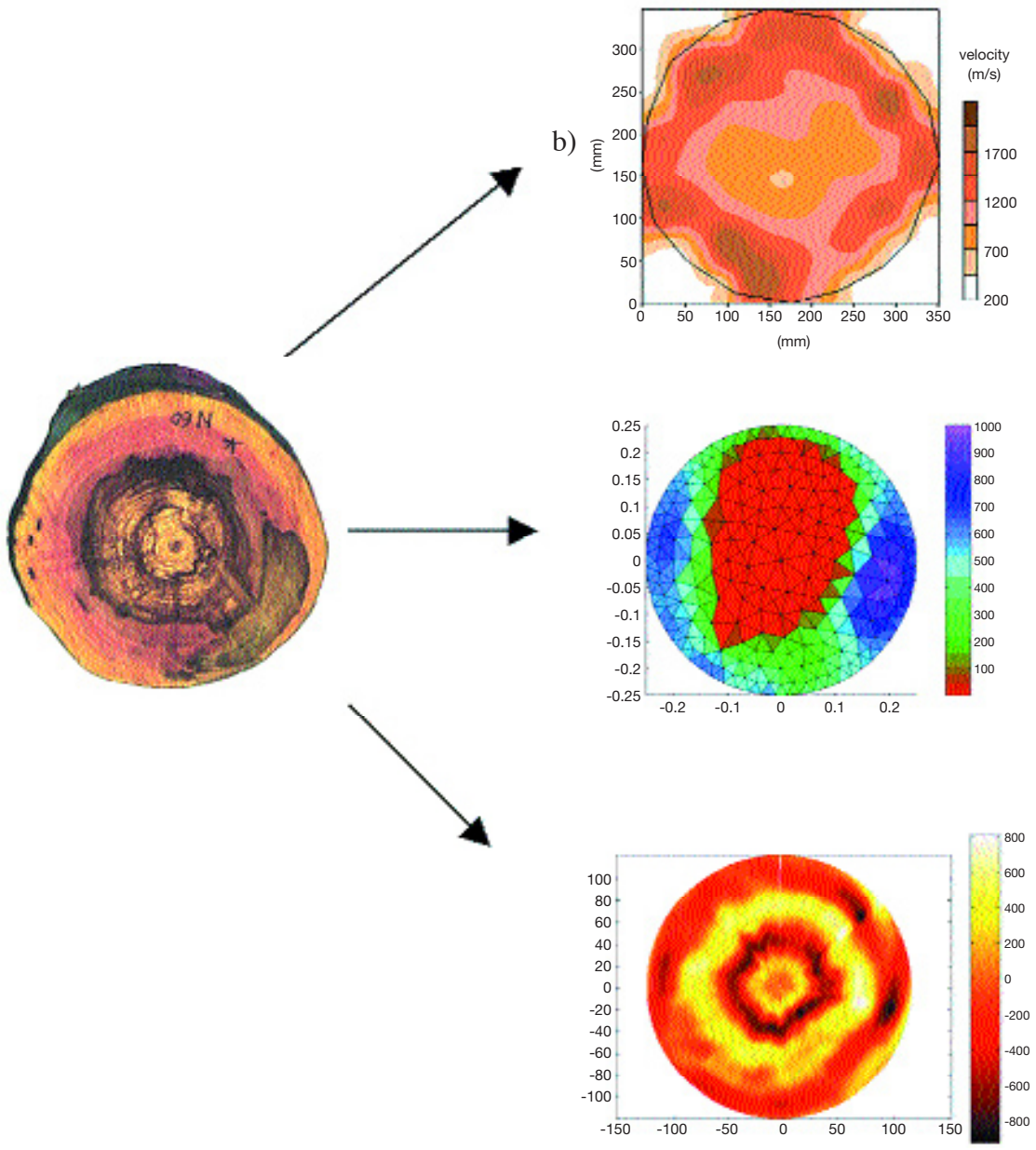

Fig. 15 - Results on a plane: a) section of the plane at 60 cm above the ground; b) ultrasonic tomography results; c) electric tomography (normalised resistivity); d) georadar polar representation (amplitude of reflection).

The pre-processing of tomographic data and the laboratory measurements have nevertheless pointed out many aspects that should be taken into account when performing tomographic acquisition and inversion. Some limits, mainly related to the actual commercial equipment, can also be underlined:

- data acquisition by single-channel instrument is quite time consuming;
- the signal-to-noise ratio is always inadequate and the first picking could, in some cases, become a quite time-consuming step;

- the statistical processing of data could supply some useful parameters and some "warnings" for image interpretation;
- the appreciable difference between radial and tangential velocity could create "ghosts" in the tomographic image due to velocity anisotropy;
- velocity values of low velocity anomalies are overestimated.

Many of the limits previously stressed are not inherent to the method proposed but are related to the fact that the equipment and the software were not specifically designed for tree applications. These limitations could, therefore, be overcome with engineering improvements involving the development of a multi-channel ultrasonic device, able to supply an amplified and sharp energising pulse, by which the acquisition could be speeded up and the signal-to-noise ratio could be improved allowing auto-picking procedures.

The last two aspects pointed out in the previous list of limitations, ghosts due to anisotropy and overestimation of velocity values in low zones, deserve further consideration.

As said before, the problem of anisotropy does not seem to hide the presence of decay. Both low velocity anomalies (due to rotting or cavities) and high velocity anomalies (due to knots) were detected with good accuracy in spite of wood anisotropy. On the contrary, tomographic images performed on healthy trees have often shown a characteristic pattern with a low velocity peripheral zone and a faster internal zone (Fig. 4). This pattern does not seem to be justified by the real distribution of the mechanical properties and could be caused by anisotropy. The main consequence of this is that tomographic images performed, considering wood as an isotropic medium, are useful for decay detection but they are not a reliable tool for the study of the mechanical properties of healthy wood.

The underestimation of the velocity decrease of decayed zones (Wielandt effect) is due to the fact that the first arrival ray paths tend to avoid low velocity regions and, therefore, the corresponding travel times do not contain information on the material within these slow areas (Nolet, 1987). This problem emerges quite often in the results of the experiments: in tomographic processing of high velocity zones, such as knots, satisfying quantitative results (Fig. 6) are always detected, while in low velocity zones, such as decay, values higher than the real ones are always assigned (Fig. 7). Even cavities inside the trunks are detected by tomographic processing but the velocity is often more than twice the velocity of ultrasonic pulse in air. This problem should always be considered during the interpretation of the results.

Some critical remarks about the usual approaches to ultrasonic and sonic measurements on trees can be also made, stressing some "warnings" that should be kept in mind performing this kind of survey:

- travel time detection very often needs signal analysis procedures, therefore, measurements based on automatic reading of pulse travel time can be affected by severe measuring errors;
- signal attenuation is strongly dependent on probe coupling and on the presence of exposed decay and therefore, this parameter can be used to diagnose the inner properties of the trunk only if the contrast of acoustic impedance of probe-bark coupling is known in all measuring points;
- the great variability of the velocity values inside the trunk section proves that data interpretation based on standard velocity values deducted by literature or by statistical analysis are very rough;

- statistical analysis of mathematical and physical resolution emphasizes that tomographic processing can supply only very poor results if the number of measurements and the signal frequency are low (as occurs in some sonic energization proposed);
- the problem of mathematical resolution should be taken into account also considering the idea of performing 3D tomographic acquisition; the number of measurements which should be carried out to obtain a reasonably small voxel size would in fact be very high, making the method not very cost-effective. Besides this, the strong anisotropy that characterises longitudinal direction properties will create many difficulties in 3D tomographic processing. In addition, two other aspects do not make the 3D approach convenient in this case. The first, sample measurements showed that longitudinal velocity seems to be a "less diagnostic" parameter for decay detection than corresponding tangential and radial velocity, second, the geometry of the investigated body (the tree) is particularly suitable for a 2D approach. If 3D results are needed they could be better obtained by assembling 2D tomographies acquired at different heights.

As far as the resistivity tomography is concerned, it should be performed according to a trade off between the situation with maximum contrast of resistivity and the minimum electrode impedance, bearing in mind that the higher the frequency used the shorter the measurement time and hence the lower the costs. A limit of resistivity tomography is, however, the possibility of infecting trees with the nails used as electrodes; in this case each set of electrodes should be used only once. The higher frequencies needed in capacitance tomography would avoid the possibility of giving images with clear differences within zones with moisture above the saturation point. On the other hand, would the aim of the tomography be to distinguish between "saturated" and "non saturated" zones, the capacitance tomography, thanks to its absolutely non-invasive character, would be preferred as diagnostic tool. The nails would in fact be substituted by plates applied to the trunk perimeter.

The radar characterisation of trunk permitted to evaluate a marked difference of electromagnetic properties between the decayed and the sound zone of wood; this is mainly related to the difference in water content.

The georadar experiments carried out on the trunk pointed out that the decayed zone are mainly associated to the decrease of the amplitude of the radar signal, due to the increase in the attenuation properties of these zones. The good correlation between the lack in signal amplitude and the decayed zone revealed by the analysis of the trunk disks are an encouragement to improve the data processing in terms of signal attenuation analysis. Tests of transillumination measurements, using two separated antennas, have proven how difficult it is to acquire good quality data at high frequency using dipole antennas, not permitting an accurate data acquisition for traveltime and attenuation tomographic data processing. On the other hand, the acquisition and data processing of a single continuous mode is very fast and guarantees an accurate detection of decayed wood on trunk with regular external surface.

References

Adjanohoun G., Guillot J.L., Lanvin J.D. and Cholat R.; 1999: *Small roundwood grading by non destructive x-rays and ultrasonic waves methods*. The e-Journal of Nondestructive Testing and Ultrasonics. www.NDT.net, **4** (11).

Bauer C., Kilbertus G. and Bucur V.; 1991: *Technique ultrasonore de caractérisation du degré d'altération des bois de hêtre et de pin soumis à l'attaque de differents champignons*. Holzforschung, **45**, 41-46.

Beall F.C.; 1996: *Application of ultrasonic technology to wood and wood-based materials*. In: 2nd Int. Conference on the development of Wood Science/Technology and Forestry, Sopron, Hungary, 10 pp.

Berndt H., Schniewind A.P. and Johnson G.C.; 1999: *High-resolution ultrasonic imaging of wood*. Wood Science and Technology, **33**, 185-198.

Berndt H., Schniewind A.P. and Johnson G.C.; 2000: *Ultrasonic energy propagation trough wood: where, when, how much*. In: Proc. 12th Int. Symposium on NDT of Wood, Sopron 13-15 Sept. 2000, pp. 57-66.

Biagi E., Gatteschi G., Masotti L. and Zanini A.; 1994: *Tomografia ad ultrasuoni per la caratterizzazione difettologica del legno*. Alta frequenza - Rivista di elettronica, **6**, 48-57.

Birchkak R., Gardner C.G., Hipp J.E. and Victor J.M.; 1974: *High dielectric constant microwave probes for sensing soil moisture*. In: Proc. Institute of Electrical and Electronics Engineers, **62**, pp. 93-98.

Blanchard R.O., Shortle W.C. and Davis W.; 1983: *Mechanism relating cambial electrical resistance to periodic growth rate of balsam fir.* Canadian Journal of Forest Research, **13**, 472-480.

Blanchard R.O. and Tattar T.A.; 1974: *Electrical properties of wood in progressive stages of discoloration and decay*. Phytopathology, **64**, 578-579.

Borsic A.; 1998: *Tomografia elettrica in bassa frequenza per il riconoscimento di discontinuità in oggetti cilindrici*. Tesi di Laurea, Politecnico di Torino, Facoltà di Ingegneria, 173 pp.

Bozhang S. and Pellerin R.F.; 1996: *Nondestructive evaluation of the degree of deterioration in wood: stress wave frequency spectrum analysis*. In: Proc. of the 10th Int. Symposium on Nondestructive Testing of Wood, August 26-28, 1996, Lausanne, Switzerland, Presses Polytechniques et Universitaires Romandes, pp. 99-115.

Brownlow White N.; 1996: *Development of phase-sensitive electrical impedance tomography for the detection of decay in wood*. PhD Thesis, University of Manchester, Institute of Science and Technology, 195 pp.

Bucur V.; 1980: *Ultrasonics, hardness and X-ray densitometric analysis of wood*. Ultrasonics, **25**, 269-275.

Bucur V.; 1995: *Acoustics of wood*. CRC Press Boca Raton, USA, 286 pp.

Bucur V.; 1999: *Acoustics as a tool for the nondestructive testing of wood*. In: Int. Symposium on NDT Contribution to the Infrastructure Safety Systems. November 22-26, 1999, Torres, Brazil., Eds. UFSM, Santa Maria Brazil.

Bucur V. and Archer R.R.; 1984: *Elastic constants for wood by an ultrasonic method*. Wood Science and Technology, **18**, 255-265.

Bucur V. and Rasolofosaon P.N.J.; 1998: *Dynamic elastic and nonlinearity in wood and rock*. Ultrasonics, **36**, 813-824.

Chambellan D., Pascal G. and Reverchon P.; 1994: *Imageur radiometrique pour le controle par défilement ou la tomodensitometrie à l'aide de photons X ou gamma*. In: 6th Conference COFREND, Nice, 1994.

Comino E., Martinis R., Nicolotti G., Sambuelli L. and Socco V.; 2000: *Low currents tomography for tree stability assessment*. In: Backhaus G.F., Balder H. and Idczak E. (eds), Int. Symposium on Plant Health in Urban Horticulture, Braunschweig 22-25 May 2000.

Comino E., Socco L.V., Martinis R., Nicolotti G. and Sambuelli L.; 2000: *Ultrasonic tomography for wood decay diagnosis*. In: Backhaus G.F., Balder H. and Idczak E. (eds), Int. Symposium on Plant Health in Urban Horticulture, Braunschweig 22-25 May 2000.

Dines K. and Lytle J.; 1979: *Computerized geophysical tomography.* In: Proc. Institute of Electrical and Electronics Engineers, **67**, pp. 1065-1073.

Divos F.; 2000: *Stress wave based tomography for tree evaluation*. In: 12th Int. Symposium on Nondestructive Testing of Wood, Sopron, 13-15 Sept. 2000. Abstract, 469 pp.

Dubbel V.V., Weihs U., Krummheuer F. and Just A.; 1999: *Neue methode zur zweidimensionalen Darstellung von Fäulen an Fichte*. AFZ/DerWald, **26**, 1422-1424.

Gilbert P.; 1972: *Iterative methods for the three-dimensional reconstruction of an object from projections*. J. Theor. Biol., **36**, 105-117.

Gill P.E., Murray W. and Wright M.H.; 1981: *Practical optimization,* Academic Press, London, 389 pp.

Giordano G.; 1981: *Tecnologia del legno*. La materia prima. **1**, UTET, Torino, 1256 pp.

Godio A., Sambuelli L. and Socco L.V.; 1999: *Geophysical techniques applied to trees assessment*. In: Proc. V E.E.G.S. European Section Meeting, Budapest, 6 - 9 Sept. IcP4, pp. 323-324.

Grootveld C.J., Seagal A. and Scarlett B.; 1998: *Regularized modified Newton-Raphson technique applied to electrical impedance tomography*. Imaging Systems Technology, **9**, 60-65.

Guddanti S. and Chan S.J.; 1998: *Replicating sawmill sawing with topsaw using CT images of a full-length hardwood log*. Forest Product Journal, **48**, 72-75.

Hruska J., Cermák J. and Sustek S.; 1999: *Mapping tree root systems with ground-penetrating radar.* Tree Physiology, **19**, 125-130.

Lawday G., Dolwin J.A., Lonsdale D. and Barnett J.R.; 2000: *Development and use of stress wave meter, to detect the presence of decay in wood blocks*. In: Proc. 12th Int. Symposium on Nondestructive Testing of Wood, Sopron 13-15 Sept. 2000, pp. 187-196.

Loke M.H. and Barker R.D.; 1996: *Rapid least-squares inversion of apparent resistivity pseudosections by a quasi-Newton method*. Geophysical Prospecting **44**, 131-152.

Mattheck C. and Breloer H.; 1994: *Field guide for visual tree assessment (VTA)*. Arboricultural J., **18**, 1-23.

McGaughey W.J. and Young R.P.; 1990: *Comparison of ART, SIRT, Least-Squares, and SVD two dimensional tomographic inversions of field data*. In: Society of Exploration Geophysicists 60th Annual Meeting, Exp. Abstr. SEG, pp. 74-77.

Menke W.; 1984: *The resolving power of cross-borehole tomography.* Geophys. Res. Lett., **11**, 105-108.

Mosig J.R., Besson J.E., Gex-Fabry M. and Gardiol F.E.; 1981: *Reflection of open-ended coaxial line and application to nondestructive measurement of materials*. Institute of Electrical and Electronics Engineers Transaction on Instrumentation and Measurement, **IM-30**, 46-51.

Nicolotti G. and Miglietta P.; 1998: *Using high-technology instruments to assess defects in trees*. Journal of Arboriculture **24**, 297-302.

Nolet G. (ed); 1987: *Seismic tomography, with applications in global seismology and exploration geophysics*. Reidel, Boston, 336 pp.

Oja J.; 1999: *X-ray measurements of properties of saw logs*. In: Doctoral Thesis, Luleå University of Technology, Skellefteå Campus, Division of Wood Technology, 124 pp.

Reynolds J.M.; 1997: *An introduction to applied and environmental geophysics*. Wiley J. and Sons, New York, 796 pp.

Ross R.J., DeGroot R.C., Nelson W.J. and Lebow P.K.; 1997: *The relationship between stress wave transmission characteristics and the compressive strength of biologically degraded wood*. Forest Products J., **47**, 89-93.

Ross R. and Pellerin R.; 1994: *Nondestructive testing for assessing wood members in structures: a review.* Gen. Tech. Rep. FPL-GTR-70. Madison, WI, 40 pp.

Rust S.; 1999: *Comparison of three methods for determining the conductive xylem area of Scots Pine (Pinus sylvestris)*. Forestry, **72**, 103-108.

Rust S. and Göcke L.; 2000: *PICUS Sonic Tomograph – a new device for nondestructive timber testing*. In: Backhaus G.F., Balder H. and Idczak E. (eds), Int. Symposium on Plant Health in Urban Horticulture, Braunschweig 22-25 May 2000.

Sandoz J.L.; 1996: *Ultrasonics solid wood evaluation in industrial applications*. In: Proc. 10th Int. Symposium on Nondestructive Testing of Wood, Lausanne (CH), 26-28 Sept. 1996, 6 pp.

Sandoz J.L., Benoit Y. and Demay L.; 2000: *Wood testing using acousto-ultrasonic*. In: Proc. 12th Int. Symposium on Nondestructive Testing of Wood, Sopron, 13-15 September. pp. 97-104.

Sandoz J.L. and Lorin P.; 1995: *K-Store et Polux. Les nouvelles technologies du poteau bois*. J. de la Construction, **12**, 8.

Schneider W.A., Ranzinger K.A., Balch A.H. and Kruse C.; 1992: *A dynamic programming approach to first arrival traveltime computation in media with arbitrary distributed velocities*. Geophysics, **57**, 39-50.

Skaar C.; 1988: *Wood-water relations*. Springer - Verlag, Heidelberg, 283 pp.

Smith K.T., Blanchard R.O. and Shortle W.C.; 1984: *Cambial electrical resistance related to number of vascular cambial cells in balsam fir.* Canadian J. of Forest Research, **14**, 950-952.

Smith K.T. and Ostrofsky W.D.; 1993: *Cambial and internal electrical resistance of red spruce trees in eight diverse stands in the northeastern United States*. Canadian J. of Forest Research, **23**, 322-326.

Smith K.T. and Shortle W.C.; 1988: *Electrical resistance and wood decay by white rot fungi*. Mycologia, **80**, 124-126.

Socco L.V., Martinis R., Comino E., Nicolotti G. and Sambuelli L.; 2000: *Open problems concerning ultrasonic tomography for wood decays diagnosis*. In: Proc. 12th Int. Symposium on Nondestructive Testing of Wood, Sopron, 13-15 Sept. 2000, Abstract 468.

Sylvia D.M. and Tattar T.A.; 1976: *Electrical resistance studies of tree cankers*. In: Proceedings of the American Phytopathological Society, 3, pp. 312.

Temnerud E. and Oja J.; 1998: *A preliminary study on unbiased volume estimation of resin pockets using stereology to interpret CT-scanned images from one spruce log*. Holz als Roh und Werkstoff, **56**, 193-200.

Tomikawa Y., Iwase Y., Arita K. and Yamada H.; 1990: *Nondestructive inspection of wooden poles using ultrasonic computed tomography*. Institute of Electrical and Electronics Engineers, Transaction on UFFC, **33**, 354-358.

Torgovnikov G.I.; 1993: *Dielectric properties of wood and wood-based materials*. Springer-Verlag, Heidelberg, 196 pp.

Turner G., Siggins A.F. and Hunt L.D.; 1993: *Ground penetrating radar-will it clear the haze at your site?* Exploration Geophysics, **24**, 819-832.

Weihs U., Dubbel V.V., Krummheuer F. and Just A.; 1999: *Die Elektrische Widerstandstomographie - Ein vielversprechendes Verfahren zur Farbkerndiagnose am stehenden Rotbuchenstamm*. Forst und Holz, **54**, 166-170.

Wilcox W.W.; 1978: *Review of the literature of the effects of early stages of decay on wood strength*. Wood and fiber, **9**, 252-257.

Wilcox W.W.; 1988: *Detection of early stages of wood decay with ultrasonic pulse velocity*. For. Prod. J., **38**, 68-73.

Zoughi R.; 1990: *Microwave nondestructive testing: theories and applications*. In: Int. Advances in Nondestructive Testing, Vol. **15**, Routledge, New York, pp. 225-288.